

# Thermal chemical conversion of high density polyethylene for the production of valuable carbon nanotubes using Ni/AAO membrane catalyst

Xiaotong Liu<sup>a</sup>, Hongman Sun<sup>a</sup>, Chunfei Wu<sup>a,b\*</sup>, Dipesh Patel<sup>a</sup>, Jun Huang<sup>c\*</sup>

<sup>a</sup> School of Engineering & Computer Sciences, University of Hull, Hull, HU6 7RX, UK

<sup>b</sup> School of Energy & Environmental Engineering, Hebei University of Technology, Tianjin, China

<sup>c</sup> School of Chemical and Biomolecular Engineering, the University of Sydney, Australia, NSW 2037

\* Corresponding authors: Tel: +44 1482466464; E-mail: c.wu@hull.ac.uk (C Wu); Tel: +86 2260435784; E-mail: Email: jun.huang@sydney.edu.au (J Huang)

**Abstract:** Thermal chemical conversion of waste plastics for syngas production is a promising alternative methods for the management of waste plastics. However, one of the challenges to facilitate the deployment of this technology is the low economic benefit of waste plastic recycling. By producing a high value carbon nanotubes (CNTs) by-product, an interesting alternative solution is provided. To further enhance the quality of CNTs produced from catalytic thermal chemical conversion of waste plastics, a template based catalyst (Ni/anodic anodic aluminium oxide–AAO) is proposed in this work. In addition, reaction temperature, Ni content and water injection were studied for their influences on the formation of CNTs on Ni/AAO using a two-stage fixed bed reactor. Various analytical methods e.g. scanning electronic microscopy (SEM) and X-ray diffraction (XRD) were used to evaluate the performance of catalyst in relation to the production of CNTs. The results show that a higher loading of Ni on AAO resulted in the formation of metal particles with various sizes, thus leading to the production of non-uniform CNTs. In addition, an optimal catalytic temperature of 700 °C is suggested for the production of CNTs. As catalyst might not be activated at 600 °C, which produced a low yield of CNTs. However, a reaction temperature of 800 °C resulted in a low yield of CNTs. Carbon deposition decreased with an increase of steam injection, but the quality of CNTs formation in relation to the uniform of CNTs seems to be improved in the presence of steam.

**Keywords:** Plastics waste; Carbon nanotubes; AAO membrane; Nickel; catalyst

## 1. Introduction

In 2015, approximately 3.7 million tonnes of plastics waste was produced in the UK <sup>1</sup>. Landfill, energy recovery and recycling are the three main treatment methods of waste plastics. Recycling of waste plastics is a high efficient method as compared to energy recovery and landfill. In particular, thermo-chemical recycling of waste plastics is a promising advanced technology. It has been reported that through high temperature pyrolysis (>800 °C) or gasification of waste plastics in the presence of catalyst, hydrogen-enriched syngas was produced <sup>2</sup>. Syngas can be directly combusted for the production of heat and power, converted to liquid fuel through Fischer-Tropsch process <sup>3</sup>. According to the recent research, the syngas (mainly CO<sub>2</sub>, CH<sub>4</sub> and CO) from wasted rubber tyres and plastics could be also used for growth of NiO nanorods, SiC nanowires and monolayer graphene via a Green-CVD method <sup>4</sup>.

For the last several decades, pyrolysis/gasification of waste plastics has been extensively studied. Park et al. <sup>5</sup> investigated pyrolysis and steam reforming of waste plastics in the presence of a Ru/ $\gamma$ -Al<sub>2</sub>O<sub>3</sub> catalyst to produce hydrogen-enriched syngas. Erkiaga et al. <sup>6</sup> studied the influences of various parameters including temperature and steam addition on the production of hydrogen and carbon conversion from gasification of high density polyethylene (HDPE), and reported around 60 vol% yield of H<sub>2</sub> (1.5 wt.% of plastics). However, gasification of waste plastics has two key challenges, including low economic profit and the deactivation of catalyst due to the deposition of coke on the surface of spent catalyst.

Recently, study on co-production of carbon nanotubes (CNTs) and hydrogen from

pyrolysis/gasification of waste plastics were investigated and developed <sup>7-9</sup>. For example, Liu et al. <sup>10</sup> converted polypropylene (PP) into multi-walled CNTs (MWCNTs) and hydrogen-rich gas. The production of MWCNTs was investigated in relation to the yield and concentration of pyrolysis gas. CNTs were initially introduced by Radushkevich and Lukyanovich in 1952, and have attracted many attentions from the early 1990s <sup>11, 12</sup>. CNTs are classified into two types, including single wall carbon nanotubes (SWCNTs) which comprise only one cylinder and multi-walls carbon nanotubes (MWCNTs) containing at least two cylinders <sup>13</sup>. CNTs has attracted a wide attention because of the extraordinary properties, and the promising potential applications <sup>13</sup>. However, the high price (~\$35/g for MWNTs, \$270/g for SWCNTs) of CNTs significantly prohibits the applications of CNTs <sup>14</sup>. Therefore, converting waste plastics into CNTs and hydrogen-enriched gases is a promising alternative to manage waste plastics, and to produce cost-effective CNTs.

Chemical vapour deposition (CVD) method is currently the most common method for the synthesis of CNTs from pyrolysis of waste plastics due to its simplicity and low cost. For example, Barbarias et al. <sup>15</sup> studied two different types of plastics including polystyrene (PS) and HDPE to produce CNTs in the presence of a Ni catalyst by using CVD method. HDPE was found to produce a higher yield of CNTs when compared to PS. Wu et al. <sup>16</sup> reported that an increase in the ratio of catalysts to plastics from 0.5 to 2 and a gasification temperature of 700 °C could improve the quality of CNTs in relation to the purity. Similar results were also found by Acomb et al <sup>17</sup>. They reported that the conversion of waste plastics into CNTs decreased from 29.1 wt. % to 13.1 wt. % when

the catalyst/plastic ratio was reduced from 1 down to 0.4. Yao et al. produced high quality of CNTs with clean hydrogen from waste plastics by Ni-Fe bimetallic catalysts<sup>18</sup>. HZSM-5 zeolite and NiO were used to convert polypropylene into multi-walled carbon nanotubes by Liu et al., and the pyrolysis and decomposition temperature were studied, respectively<sup>10</sup>. The CNTs yield reached to the highest at the decomposition temperature of 700°C. Similar temperature study was also carried out by Mishra et al, a waste polypropylene was used as carbon source for CNTs synthesis with nickel catalysts, 800°C was found to produce the purest CNTs<sup>19</sup>.

However, CNTs produced from catalytic thermo-chemical conversion of waste plastics are generally with poor quality due to the use of granular catalysts e.g. uncontrollable diameter, non-uniform thickness or length of CNTs. The catalysts used for CVD synthesis of CNTs formation normally consist of transition metal and substrates. Various substrates have been widely used for CVD of CNTs synthesis, such as silicon dioxide, alumina, quartz, calcium carbonate, zeolite and etc.<sup>20 21</sup>. The surface morphology and texture properties of substrates were reported to affect the yield and the quality of CNTs formation<sup>22</sup>. The physical and chemical interactions between the substrate and active metals are also important factors during CNTs synthesis process.

In order to produce high quality CNTs in relation to the uniform distribution of CNTs diameter length and wall thickness<sup>23</sup>, template controlled CNTs production has been studied. For example, Ni-coated glass was successfully used as a template by Ren et al.<sup>24</sup> to synthesise ordered CNTs from acetylene at above 700 °C using plasma-enhanced hot filament CVD method. Che et al.<sup>25</sup> prepared graphitic carbon nanotubes within a

porous alumina template from ethylene and pyrene using a CVD method in the presence of Ni-based catalysts. The template method was introduced to provide a support with uniform structure for the growth of CNTs.

Anodic aluminium oxide (AAO) membrane which was used in this paper, has been studied as a template for CNTs growth using pure carbon source<sup>25-27</sup>. AAO membrane presents several advantageous features compared to granular catalysts, such as achievable pore diameter, lengths and inner pore distances. These features could lead to the production of CNTs with a high morphological quality. In addition, AAO can be easily dissolved in alkaline or acidic during the separation of CNTs<sup>28</sup>. Kyotani et al.<sup>29</sup> produced CNTs at 800 °C on AAO membrane from pyrolytic propylene, the CNTs presented with an outer diameter of 30 nm and a length of 60 nm corresponding to the channel diameter and the thickness of AAO membrane, respectively. Chen et al.<sup>30</sup> synthesized CNTs by casting thin films of polyacrylonitrile and polystyrene-block-polyacrylonitrile within AAO membrane followed by pyrolysis. They found that the wall thickness of the produced CNTs was controlled by the concentration of the precursor solution. The effect of reaction gases (CO and C<sub>2</sub>H<sub>2</sub>) on the formation of CNTs has been studied by Jeong et al.<sup>27</sup> with a Co-based AAO catalysts, CNTs synthesized in the presence of CO showed a lower growth rate as compared to C<sub>2</sub>H<sub>2</sub>. In addition, key parameters such as deposition time, temperature and precursor gas flow rate have been studied by Golshadi et al.<sup>31</sup> to synthesize CNTs from a 30/70 (vol%) ethylene/helium gas mixture using AAO-based catalysts. They found that longer deposition time and higher reaction temperature could enhance the yield and the

thickness of CNTs.

However, most previous studies focused on the production of CNTs on AAO based catalysts used pure carbon sources. There are only a few publications that have reported using waste plastics as feedstock in the presence AAO template catalyst to synthesize CNTs<sup>27</sup>. Therefore, in this work Ni-based AAO catalysts were investigated to produce CNTs from pyrolysis/gasification of waste plastics aiming to generate high quality CNTs with uniform distributions of diameters. In addition, the influence of metal loading, reaction temperature and steam injection were studied to optimize the process conditions.

## **2. Experimental**

### **2.1 Materials**

Waste high density polyethylene plastics (HDPE) with a diameter around 2 mm were obtained from Poli Plastic Pellets Ltd., UK. AAO membrane used in this study was from Whatman (Anodisc 13) with a 200 nm nominal pore diameter and a 60  $\mu\text{m}$  thickness. Initially, the required amount of nickel nitrate hexahydrate  $\text{Ni}(\text{NO}_3)_2 \cdot 6\text{H}_2\text{O}$  (0.1, 0.5, 1 or 2  $\text{mol L}^{-1}$ ) was dissolved in ethanol. Nickel precursor was doped on AAO membrane by dropping the precursor on the surface of AAO membrane. Filter paper was used to absorb the extra solvent left on the AAO membrane avoiding accumulation of Ni particles on the AAO membrane surface. The obtained Ni/AAO membrane precursor was dried in an oven at 100  $^\circ\text{C}$  for 24 hrs, then calcined in air for 3 hrs at 700  $^\circ\text{C}$  with a 10  $^\circ\text{C min}^{-1}$  heating rate. It was noted that the Ni/AAO catalysts prepared

from using 0, 0.1, 0.5, 1.0 and 2.0 mol L<sup>-1</sup> of Ni (NO<sub>3</sub>)<sub>2</sub>.6H<sub>2</sub>O were assigned as original AAO, 0.1/AAO, 0.5/AAO, 1.0/AAO and 2.0/AAO catalysts, respectively.

## 2.2 CNTs synthesis from catalytic thermo-chemical conversion of waste plastics

A two-stage catalytic thermo-chemical conversion reaction system (Fig. 1) consisting of a plastic pyrolysis stage and a catalytic gasification stage was used in this study. For each experiment, about 1 g of HDPE was pyrolysed at temperature of 500 °C in the first stage, and the produced vapours representing a hydrocarbon source passed to the second reaction stage where a bed of the Ni/AAO catalyst was located. N<sub>2</sub> was used as carrier gas with 100 mL min<sup>-1</sup> flow rate. It was to be noted that the catalytic reactor (2<sup>nd</sup> stage) was preheated to a desired catalytic temperature (600°C, 700°C, and 800°C) prior the heating of the 1<sup>st</sup> stage (pyrolysis). 1g of conditioning catalysts (10 wt. % Ni/Al<sub>2</sub>O<sub>3</sub>), which placed on the top of the Ni/AAO catalyst, was used to modify the hydrocarbon sources before the growth of CNTs on the AAO catalysts. This layer of conditioning catalyst was used to investigate other experimental factors e.g. reaction temperature. However, the reacted conditioning catalyst was not analysed in this work, which focused on the Ni/AAO catalyst for CNTs production. The total reaction time was 60 mins. The system was then slowly cooled down to the room temperature with continuous N<sub>2</sub> gas flow rate of 100 mL min<sup>-1</sup>. The spent Ni/AAO catalysts with produced CNTs were collected for further characterizations.

The effect of gasification temperature, steam injection and the content of Ni on AAO membrane were studied in relation to their influence on the growth of CNTs. It was

noted that gas and liquid product that were produced as part of this work were not analysed, as the main aim of the research work was to investigate the influence of template catalyst on the production of CNTs in relation to the quality of CNTs.

### 2.3 Sample characterizations

A high resolution scanning electron microscope (SEM) Stereoscan 360 and a transmission electron microscope (TEM) JEOL 2010 were used to analyse the morphologies of the fresh catalysts. Elemental analysis of the fresh Ni/AAO catalysts were studied by dispersive X-ray spectroscopy (SEM/EDX). Fresh Ni/AAO catalysts were also characterized by powder X-ray diffraction (XRD), and the data was further analyzed with Stoe IPDS2 software. In addition, the particle size of NiO was calculated from XRD results using Highscore software.

CNTs formed on the reacted Ni/AAO catalysts were also investigated by SEM and TEM. The distribution of CNTs diameters according to SEM results was determined using an Image-J software. Temperature programmed oxidation (TPO) of the reacted Ni/AAO catalysts was carried out to obtain the information of carbon formation (e.g. weight loss and oxidation temperature) on the reacted catalysts. For each experiment, around 5 mg reacted Ni/AAO catalysts was placed inside the TGA (TA Instruments, SDT-Q600), which was heated from room temperature up to 800 °C with an air flow rate of 100 mL min<sup>-1</sup>.

### **3. Role of AAO membrane substrate**

AAO membrane was used as substrate of catalyst in this study. The original AAO without nickel loading was identified by XRD diffraction (Fig.2), the original AAO membrane showed the presence of three main diffraction peaks at around 43°, 50° and 74°, respectively. These three peaks were identified as Al<sub>2</sub>O<sub>3</sub><sup>32 33</sup> and marked as ‘AAO’ peaks for the following XRD analysis. According to SME analysis, a large number of uniform pores (Fig. 2) and highly ordered nanochannels (Fig. S1) could be observed on the surface of the AAO membrane without nickel loading. The structure of the AAO membrane used and reported in this study was consistent with AAO templates used in other studies<sup>26, 27, 34</sup>.

Fresh Ni/AAO catalysts with four different Ni loadings were characterized by XRD (Fig S2), EDX (Table S1), SEM (Fig. 3A-D) and TEM (Fig.3 i-v). The diffraction peaks of NiO were clearly observed at 37°, 62°, 75° and 78°<sup>35</sup> for the 0.5/AAO, 1.0/AAO, and 2.0/AAO (Fig. S2 B-D), respectively. Only one weak diffraction peak at 62° was observed in relation to NiO for the 0.1/AAO (Fig. S2 A). It is suggested the NiO particles in the 0.1/AAO were too small to be detected by XRD. However, the EDX analysis (Table S1) confirmed the presence of Ni on the surface of the 0.1/AAO. Semi-quantitative analysis using EDX showed that Ni content was increased from 2.4 to 28.2 wt. % with increasing Ni concentration in the precursor during catalyst preparation. Element of O was originated from NiO and AAO, and Al was from AAO. According to the TEM results (Fig.3 i-v), the particle size of NiO for the 0.1/AAO (Fig.3 i) was hardly observed, which was consistent with the XDR results. The NiO diameter was increased from around 20 nm to over 50 nm when the catalyst was changed from the

0.5/AAO to the 2.0/AAO. In addition, various sizes of NiO particles (5-60nm) were observed on the 2.0/AAO. According to the SEM results (Fig.3 A-D), the formation of large NiO particles would occur more on the AAO surface rather than the inner channel, resulting in covering and blocking the pores on the surfaces. The blockage of AAO pores with NiO particles is particularly observed on the surface of the 1.0/AAO and the 2.0/AAO as shown in Fig. 3. Ordered pores could still be clearly observed on surface of the 0.1/AAO and the 0.5/AAO (Fig. 3A and 3B). The particle size of NiO calculated from the XRD analysis is shown in Table 1. The NiO particle sizes are consistent with the ones shown in the TEM results. The catalytic particle size was too small to be analysed through XRD, while around 32.6 nm of NiO particles are obtained for the 0.5/AAO, and larger particle sizes of NiO were observed on the 1.0/AAO (36.9 nm) and the 2.0/AAO catalyst (47.7 nm).

It is suggested that the regular pores and ordered channels of AAO could control the diameters of NiO loaded inside the membrane when the Ni loading was low (e.g. the 0.1/AAO). However, when Ni content was further increased (e.g. the 1.0/AAO), the membrane could no longer control the size of NiO particles. Therefore, a larger range of diameters of NiO appeared. The CNTs diameter was reported highly depending on the sizes of active metals from our previous study <sup>36</sup>. Therefore, the AAO used in this study aims to control the active metal sizes, in order to produce a high quality of CNTs with uniform diameter distribution.

#### **4. Production of CNTs**

Three reaction parameters using Ni/AAO membrane catalysts were investigated in relation to their effect on the formation of CNTs from waste plastics. Table 2 is a summary of different experimental parameters (Ni content, reaction temperature, and steam addition) and the information of carbon formation (amount of amorphous carbon, filamentous carbon and CNTs average diameter). When the effect of Ni content was studied, thermo-chemical conversion of waste HDPE was carried out in the presence of Ni/AAO catalyst with four different Ni contents (0.1, 0.5, 1.0 and 2.0) at 700°C. When the reaction temperature was studied, the 0.1/AAO catalyst was used to investigate the influence of reaction temperature (600 °C, 700 °C and 800 °C) on the formation of CNTs. The effect of water presence was studied with three different flow rates of 0, 2 and 5 mL h<sup>-1</sup> with the 0.1/AAO catalyst; thus the total amount of water injected into the reactor was 0, 2, and 5 ml, respectively.

In Table 2, the produced amorphous and filamentous carbons were calculated according to TGA analysis under air (TGA-TPO), as shown in Fig. S3, S4, and S5. TGA-TPO analysis of the spent catalyst was carried out to obtain the quantification of the formed carbons on the reacted catalyst, and also to discuss the oxidation temperature of the formed CNTs. It is assumed that the oxidation temperature below 550 °C was assigned to amorphous carbons and the oxidation above 550 °C in TPO was assigned to filamentous carbon (assumed as CNTs in this work)<sup>37</sup>. The fractions of the two different types of carbon are summarized in Table 2. The carbon fraction/yield was obtained by the weight in relation to carbons divided by the weight of reacted catalyst.

The quality of CNTs is discussed mainly according to the distribution of CNTs diameter.

The average diameter of CNTs was calculated based on the SEM results and was summarized in Table 2 (shown in Fig. S6, S7 and S8). The standard deviation (SD) number is used as the factor which identifies the quality of CNTs in this study. A smaller SD indicates a better quality of the produced CNTs.

#### 4.1 Effect of Ni content on the production of CNTs

In this section, thermo-chemical conversion of waste HDPE was investigated in the presence of Ni/AAO catalyst with different Ni contents. Table 2 shows that the total carbon deposition was increased with the increase of Ni loading, indicating that the formation of carbons was enhanced. The fraction of amorphous carbons was also increased with the increase of Ni content, as the availability of Ni-based particles was increased. Ni was the main active site for C-C and C-H bond cleavage to enhance the production of carbons<sup>38</sup>. Higher metal loading was reported to enhance the dehydrogenation of C<sub>2</sub> hydrocarbons to form CNTs<sup>39</sup>. Wu et al.<sup>40</sup> found that a comparatively lower amount of carbon deposition but a higher quality of CNTs was obtained when the Ni content in catalyst was reduced.

The quality of CNTs derived from the spent Ni/AAO catalysts with different Ni loadings were analysed by SEM. The images of surface and cross-section of the reacted Ni/AAO catalysts are shown in Fig. 4 and Fig.S9, respectively. Filamentous carbons were clearly produced in the presence of Ni-based catalyst (Figs. 4A-D). For the 0.1/AAO, 0.5/AAO and 1.0/AAO catalysts, filamentous carbons are observed on the surface (Fig. 4) and in the channels (Fig. S9) of AAO. It seems that there are a large

amount of amorphous carbons with short and un-uniform tube structure covered on the surface of the 2.0/AAO catalyst; this is consistent with that a large fraction of amorphous carbons is calculated from TPO analysis (Table 2). TEM results (Fig. 5) further prove that most of the filamentous carbons are CNTs.

In this study, the mechanism of CNTs synthesis with AAO based catalyst was summarized in Fig. 6, combining with SEM cross-section images of the reacted 0.1/AAO. AAO membrane with two-side open was used in this study (Fig. S1). The diameter of NiO particles in the Ni-based catalysts in this study was around 20–50 nm (Fig. 3 and Table 1), which was much smaller than the pore size of the AAO used (200 nm). It is indicated that many NiO particles could be located inside the pores, as shown in Fig. 6A. In addition, the growth of CNTs was reported could be sustained and reached the outside of the pores<sup>27</sup>. Therefore, many CNTs could be produced inside and outside the pores of AAO (Fig. 6B).

The distribution of CNTs diameters was analysed, and the results were summarized in Table 2 and Fig.7. It is demonstrated that the CNTs produced from the 0.1/AAO catalyst have the smallest average diameter of 26.7 nm and a deviation of 4.0 nm. The CNTs produced from the 0.5/AAO catalyst showed the largest deviation of average diameter (14.2 nm). The 2.0/AAO catalyst produced CNTs with the largest average diameter of 54.1 nm, which is corresponding to the size of metal particles as shown in the TEM results of Fig. 3v. It can be noticed that the diameter of CNTs is increased with an increase of Ni content (Fig. 7). It was reported that the growth of CNTs was governed by the diameter of metals<sup>8, 41-43</sup>. Sinnott et al.<sup>44</sup> studied CNTs growth from methane

with Fe/C based catalysts. They found that a lower metal content produced a smaller average diameter and a narrower diameter distribution of CNTs. Takenaka et al.<sup>45</sup> reported that the diameter of Fe-based particles was increased with an increase of metal loading, resulting in a production of non-uniform CNTs. Other researchers have also reported that metal particles such as Ni, Fe, and Co had a proportionally relationship with the diameter of produced CNTs<sup>22, 46-49</sup>. Therefore, uniform distributed metal particles are important to produce high quality CNTs in relation to the distribution of CNTs diameters. It is suggested that an AAO substrate could contribute to the uniform production of CNTs.

Although the 1.0/AAO and 2.0/AAO catalysts generated a higher carbon yield compared to the 0.1/AAO and 0.5/AAO catalysts, the 0.1/AAO catalyst produced a higher quality of CNTs in relation to the purity (less amorphous carbons) and a uniform distribution of the diameter of CNTs (Table 2). Therefore, the 0.1/AAO catalyst was used for further studies in this work.

#### 4.2 Effect of reaction temperature on the production of CNTs

The 0.1/AAO catalyst was used to investigate the effect of reaction temperature (600 °C, 700 °C and 800 °C) on the formation of CNTs. SEM analysis (Fig. 8) was carried out on the reacted catalysts. CNTs could be clearly observed on the reacted catalysts derived at reaction temperatures of 600 °C and 700 °C. However, less CNTs could be found when the reaction temperature was 800 °C (Fig. 8C). In addition, at 800 °C, the AAO membrane was cracked, as shown on the surface (Fig. 8C) and cross-section (Fig.

8D).

The distribution of the diameter of CNTs was analysed to further determine the quality of CNTs produced at different temperatures. The results are shown in Table 2. The diameter of CNTs was increased from  $26.2 \pm 6.6$  nm to  $33.5 \pm 5.6$  nm when the reaction temperature was increased from 600 °C to 700 °C. The average diameter of CNTs formed at 800 °C was around 27.2 nm with 7.2 nm deviation which is the largest among the three temperatures. This might be caused by the fracture of the AAO membrane at such high temperature. Reaction temperature was reported as a dominating factor influencing the morphology of CNTs by Kumar and Ando <sup>50</sup>, who found that the diameter range of CNTs was increased from 5-10 nm to 10-80 nm with the increase of reaction temperature from 550 °C to 1000 °C as the metal atoms of catalysts agglomerated to bigger clusters at high temperature. It is suggested that the reaction of vapour deposition was enhanced with the increase of reaction temperature, causing faster carbon deposition and resulting in the production of thicker CNTs <sup>31</sup>.

The yield and types of carbon deposition was further determined by TGA analysis (Fig. 9 and Fig. S4). As summarized in Table 2, the yield of carbon was increased with the increase of reaction temperature from 600 to 700 °C. Two oxidation peaks at around 300°C and 450°C are assigned as the oxidation of heavy hydrocarbons which were deposited on the surface of the reacted catalysts. The total carbon yield obtained at 700 °C was nearly three times higher than the carbon yield obtained at 600 °C, indicating that much more CNTs were produced at 700 °C. It is noted that an oxidation temperature at around 680 °C for the reacted catalyst obtained at reaction temperature

of 800 °C. This oxidation peak might be the oxidation of highly graphite carbons, which are not preferred in this work, as CNTs are barely observed from SEM analysis (Fig. 8 C). In addition, the deformation of AAO support at reaction temperature of 800 °C indicates that this temperature is not suitable for CNTs production from waste plastics. Thus carbon production at 800 °C are not presented in Table 2.

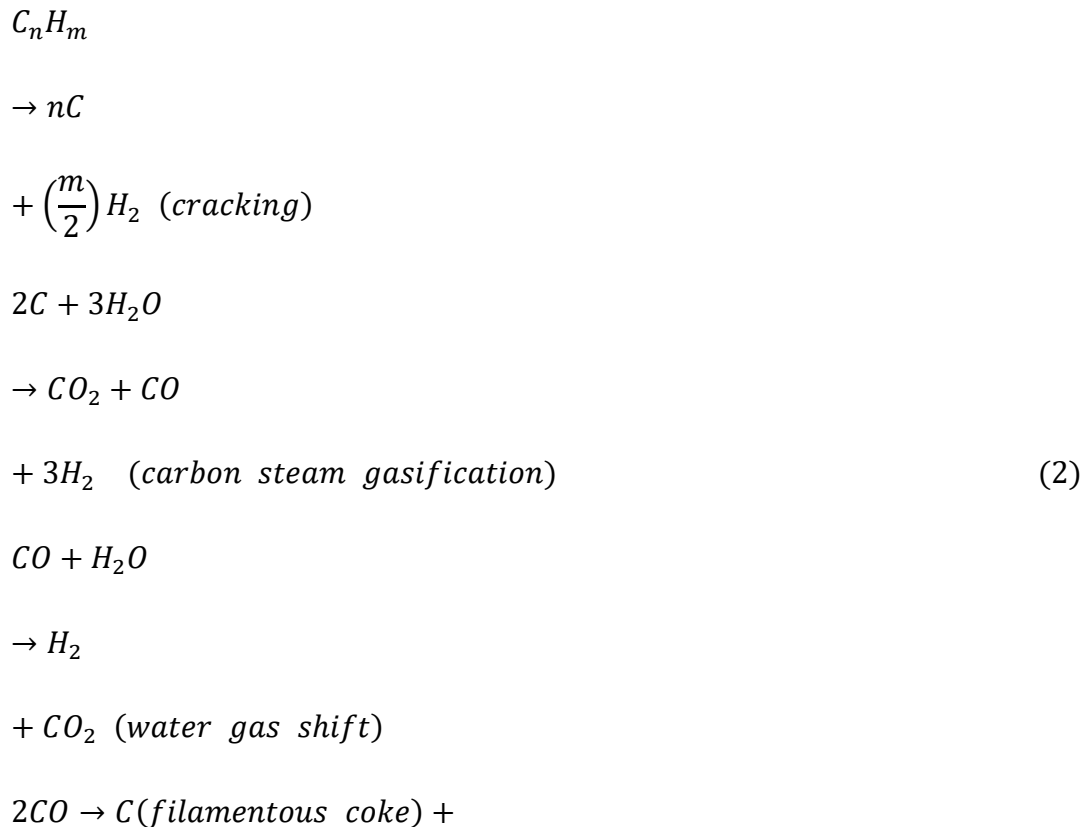
The influence of reaction temperature on the formation of CNTs has also been reported by other researchers. For example, Acomb et al.<sup>17</sup> studied the effect of temperature (700, 800, and 900 °C) on the growth of CNTs growth using a low density polyethylene and a Fe/Al<sub>2</sub>O<sub>3</sub> catalyst. They found that the yield and the quality of CNTs were improved with the increase of reaction temperature. Wu and Williams<sup>16</sup> also reported that more reactive carbons were produced at higher temperature from the gasification of waste plastics. Mishra et al.<sup>19</sup> used waste polypropylene as a precursor for synthesizing CNTs by CVD method with a nickel-based catalyst. They reported that a high degree of impurity and irregularities of CNTs was obtained at 600 °C and 700 °C. The quality of CNTs in relation to the purity and uniformity was enhanced when the reaction temperature was increased to 900 °C. In addition, a reaction temperature higher than 500 °C was suggested for the synthesis of CNTs<sup>51-53</sup>. However, the selection of reaction temperature for the growth of CNTs should also be related to other process conditions e.g. feedstock and catalyst. For instance, it was indicated that CNTs were produced at temperature higher than 1000 °C using ethanol and ferrocene as feedstock<sup>54</sup>, while no CNTs were formed at high temperature of 1000 °C from acetylene as a feedstock<sup>55-57</sup>.

Similar AAO catalysts were studied by Golshadi et al.<sup>31</sup> to investigate the influence of reaction temperature of 650, 700, 750 and 800 °C, using ethylene/helium gas mixture. At 750–800 °C, a layer of amorphous carbon was formed, prohibiting the diffusion of hydrocarbon gases, resulting in a decrease of CNTs formation. The authors suggested that 650–700 °C was an optimal temperature for CNTs growth using AAO based catalyst. This is consistent with this work confirming that 700 °C is preferable for the growth of CNTs. Similar result was also reported by Li et al.<sup>58</sup>. They reported that the yield of CNTs was changed with increasing temperature from 500 to 800 °C and that the maximum yield was obtained at 700 °C by using PP as feedstock and HZSM-5 zeolite as a catalyst. Furthermore, higher temperature was reported to cause the deformation or the sintering of catalyst, and the formation of amorphous carbons. Park et al.<sup>5</sup> found that high temperature could lead to an increase of the deposition of amorphous carbons on the surface of catalyst particles to deactivate catalysts. Therefore, in this work, 700 °C is suggested to be an optimal temperature for the production of CNTs. 600 °C is too low in relation to the thermodynamics of carbon formation reactions, while 800 °C is too high to crack the AAO catalyst and also to form a large amount of un-desired amorphous carbons.

#### 4.3 Effect of steam addition on the production of CNTs

Water was reported as a catalytic enhancer to improve the quality of CNTs<sup>59</sup>. In this study, water with three different flow rates of 0, 2 and 5 mL h<sup>-1</sup> was injected into the system to investigate the effect of steam on CNTs synthesis. The results were analysed

by SEM as shown in Fig. 10. DTG-TPO results are presented in Fig. 11. The key reactions of catalytic pyrolysis of plastics waste with steam injection are shown by Reactions 1–4. Initially, the hydrocarbons derived from plastics decomposition are cracked into carbon and hydrogen (Reaction 1). In the presence of steam, water reacts with deposited carbons to produce CO<sub>2</sub>, CO and H<sub>2</sub> (Reaction 2). Therefore, hydrogen and carbon dioxide in the gas could be increased with an increase of steam addition. The introduction of steam into plastic gasification has been widely reported to enhance the production of CO and H<sub>2</sub><sup>17, 60</sup>. According to the study from Barbarias et al.<sup>61</sup>, CO could further promote carbon growth, however, CO could also be transformed to CO<sub>2</sub> by water gas shift (Reaction 3) with the addition of water. Therefore, the decomposition of CO into carbon could be prohibited (Reaction 4).



$CO_2$  (boudouard reaction) (4)

SEM results (Fig. 10) of the reacted Ni/AAO catalysts derived from using 2 and 5 mL h<sup>-1</sup> of water steam injection were studied. Long and thin uniform CNTs on the surface of reacted catalyst have been observed. According to the SEM results, it is difficult to find the differences of CNTs produced between without steam (Fig. 4A), with 2 mL h<sup>-1</sup> steam (Fig. 10A) and 5 mL h<sup>-1</sup> steam (Fig. 10B). However, the diameter distribution analysis shows that the average diameter of CNTs is decreased with an increase of the steam flow rate from 2 mL h<sup>-1</sup> to 5 mL h<sup>-1</sup>. The average diameter of CNTs is decreased to 29.7 ± 5.7 nm and 21.9 ± 3.9 nm, when 2, and 5 mL h<sup>-1</sup> of steam were used, respectively, compared to an average diameter of CNTs of 33.5 ± 5.6 nm with no steam injection. The deviation of CNTs diameter is similar for the CNTs produced with 0 and 2 mL h<sup>-1</sup> water injection. This deviation decreased to 3.9 nm as the steam injection was increased to 5 mL h<sup>-1</sup>. It is suggested that the quality of CNTs could be improved with the increase of water injection in the process of catalytic steam conversion of waste plastics. The amorphous carbons were known to encapsulate the reactive catalytic sites and influence the quality of the formed CNTs<sup>37</sup>. Amorphous carbons could be etched away through weak oxidation reactions with an appropriate amount of steam to enhance the continuous growth of CNTs. For example, water-assisted CNTs production was carried out on different catalysts (Fe, Al/Fe, Al<sub>2</sub>O<sub>3</sub>/Fe, and Al<sub>2</sub>O<sub>3</sub>/Co on Si wafers, quartz and metal foils)<sup>62</sup>. Also Ago et al.<sup>63</sup> generated CNTs from methane with Ni, Fe, and Co/MgO catalysts. Ago and co-workers<sup>63</sup> reported that water injection prolonged the catalyst lifetime and enhanced the morphology of CNTs.

However, it is shown an obviously decrease of carbon deposition with increasing steam injection. 10% carbon formation without steam injection is obtained in relation to the weight of used catalyst. The yield of carbon was decreased to around 4.1% when the steam injection rate was 2 mL h<sup>-1</sup>, and was further decreased to less than 2.5% with the increasing steam injection to 5 mL h<sup>-1</sup>. It is suggested that the amount of steam injected into the reactor might be higher than the optimum value. It was reported that over injection of steam could increase carbon steam gasification (Reaction 2), resulting in a reduction of carbon yield <sup>64</sup>. Lee et al. <sup>65</sup> pointed out that the excess steam would limit the supply of carbon sources reaching the catalytic active sites, due to the reduced diffusion of carbon. Liu et al. <sup>66</sup> studied the effect of wet argon flow rate of 0 to 700 cm<sup>3</sup> min<sup>-1</sup> at standard temperature and pressure (scm) on CNTs growth from m-xylene using SiO<sub>2</sub> based catalyst. They found that the flow rate of wet argon in the range of 100–150 scm performed best for CNTs formation. With the introduction of excess steam, low quality of CNTs was produced because the diffusion and penetration of hydrocarbons through the nanotube bundles was reduced making it difficult for hydrocarbon molecules to reach catalytic sites for CNTs growth. Hu et al. <sup>67</sup> prepared vertically-aligned CNTs by water assisted CVD using a Mo/Fe/Al based catalyst from a C<sub>2</sub>H<sub>4</sub> and H<sub>2</sub> gas mixture. They reported that the best CNTs were found at 100 scm water vapour and that the formation of CNTs was reduced as the vapour was increased to over 150 scm.

In addition, the excess steam would largely enhance the oxidation of catalytic metal, consequently, deactivating the catalyst for the formation of CNTs. Furthermore, the

0.1/AAO catalyst contained a small amount of Ni (~2.4 wt.% according to EDX). Therefore, when more steam was injected, a small amount of active Ni catalysts might be oxidized in the process to lose the catalytic activity for CNTs growth. Yamada et al<sup>68</sup> reported that water could oxidize metal catalyst, causing the deactivation of CNTs formation.

## 5. Conclusions

Waste plastics was processed and converted into carbon nanotubes. This work focused on the formation of CNTs using anodic aluminum oxide membrane AAO as a support in order to improve the quality of CNTs in relation to the homogeneous properties (diameter distribution). The main results are concluded as follows:

(1) An increase of Ni content on Ni/AAO (Ni precursor concentration was increased from 0.1 to 2.0 mol L<sup>-1</sup>) resulted in the accumulation of metal particles on the surface of the AAO membrane. As a result, more amorphous carbons were produced. 0.1 mol L<sup>-1</sup> of Ni solution (catalyst precursor) assigned as 0.1/AAO is suggested to produce high quality CNTs in relation to the uniform distribution of diameter of CNTs.

(2) An optimal catalytic temperature of 700 °C is suggested in this work. 600 °C was too low to activate catalyst resulting in a low yield of CNTs, while 800 °C might cause the sintering of Ni-based particles resulting in the production of a large fraction of amorphous carbons which are not preferred in this work.

(3) An increase of steam injection is suggested to enhance the quality of CNTs formed on the Ni/AAO catalyst, but resulted in a large decrease on CNTs production.

## Acknowledgement

The authors would like to thank The University of Hull (UK) and Hebei University of Technology (China) for the financial support for this research work.

## References

1. WRAP, Plastics Market Situation Report. **Spring 2016**.
2. Al-Salem, S. M.; Lettieri, P.; Baeyens, J., Recycling and recovery routes of plastic solid waste (PSW): A review. *Waste Management* **2009**, 29, (10), 2625-2643.
3. Gershman, B. B., Inc., Gasification of Non-Recycled Plastics From Municipal Solid Waste In the United States. *solid waste management consultants* **2013**, GBB/12038, (1).
4. You, Y.; Mayyas, M.; Xu, S.; Mansuri, I.; Gaikwad, V.; Munroe, P.; Sahajwalla, V.; Joshi, R. K., Growth of NiO nanorods, SiC nanowires and monolayer graphene via a CVD method. *Green Chemistry* **2017**, 19, (23), 5599-5607.
5. Park, Y.; Namioka, T.; Sakamoto, S.; Min, T.-j.; Roh, S.-a.; Yoshikawa, K., Optimum operating conditions for a two-stage gasification process fueled by polypropylene by means of continuous reactor over ruthenium catalyst. *Fuel Processing Technology* **2010**, 91, (8), 951-957.
6. Erkiaga, A.; Lopez, G.; Amutio, M.; Bilbao, J.; Olazar, M., Syngas from steam gasification of polyethylene in a conical spouted bed reactor. *Fuel* **2013**, 109, 461-469.
7. Wu, C.; Nahil, M. A.; Miskolczi, N.; Huang, J.; Williams, P. T., Processing Real-

World Waste Plastics by Pyrolysis-Reforming for Hydrogen and High-Value Carbon Nanotubes. *Environmental Science & Technology* **2014**, 48, (1), 819-826.

8. Wu, C.; Dong, L.; Onwudili, J.; Williams, P. T.; Huang, J., Effect of Ni Particle Location within the Mesoporous MCM-41 Support for Hydrogen Production from the Catalytic Gasification of Biomass. *ACS Sustainable Chemistry & Engineering* **2013**, 1, (9), 1083-1091.

9. Wu, C.; Williams, P. T., Ni/CeO<sub>2</sub>/ZSM-5 catalysts for the production of hydrogen from the pyrolysis–gasification of polypropylene. *International Journal of Hydrogen Energy* **2009**, 34, (15), 6242-6252.

10. Liu, J.; Jiang, Z.; Yu, H.; Tang, T., Catalytic pyrolysis of polypropylene to synthesize carbon nanotubes and hydrogen through a two-stage process. *Polymer Degradation and Stability* **2011**, 96, (10), 1711-1719.

11. L.V. Radushkevich, V. M. O. L., Structure ugleroda, obrazujucesja pri termiceskom razlozenii okisi ugleroda na zeleznom kontakte. *Zurn Fisic Chim.* **1952**, 26, 88-95.

12. Iijima, S., Helical microtubules of graphitic carbon. *Nature* **1991**, 354, 56-58.

13. Trojanowicz, M., Analytical applications of carbon nanotubes: a review. *TrAC Trends in Analytical Chemistry* **2006**, 25, (5), 480-489.

14. Dasgupta, K.; Joshi, J. B.; Banerjee, S., Fluidized bed synthesis of carbon nanotubes – A review. *Chemical Engineering Journal* **2011**, 171, (3), 841-869.

15. Barbarias, I.; Lopez, G.; Artetxe, M.; Arregi, A.; Santamaria, L.; Bilbao, J.; Olazar, M., Pyrolysis and in-line catalytic steam reforming of polystyrene through a two-step

reaction system. *Journal of Analytical and Applied Pyrolysis* **2016**, 122, 502-510.

16. Wu, C.; Williams, P. T., Pyrolysis–gasification of post-consumer municipal solid plastic waste for hydrogen production. *International Journal of Hydrogen Energy* **2010**, 35, (3), 949-957.

17. Acomb, J. C.; Wu, C.; Williams, P. T., Effect of growth temperature and feedstock:catalyst ratio on the production of carbon nanotubes and hydrogen from the pyrolysis of waste plastics. *Journal of Analytical and Applied Pyrolysis* **2015**, 113, 231-238.

18. Yao, D.; Wu, C.; Yang, H.; Zhang, Y.; Nahil, M. A.; Chen, Y.; Williams, P. T.; Chen, H., Co-production of hydrogen and carbon nanotubes from catalytic pyrolysis of waste plastics on Ni-Fe bimetallic catalyst. *Energy Conversion and Management* **2017**, 148, (Supplement C), 692-700.

19. Mishra, N.; Das, G.; Ansaldo, A.; Genovese, A.; Malerba, M.; Povia, M.; Ricci, D.; Di Fabrizio, E.; Di Zitti, E.; Sharon, M.; Sharon, M., Pyrolysis of waste polypropylene for the synthesis of carbon nanotubes. *Journal of Analytical and Applied Pyrolysis* **2012**, 94, 91-98.

20. Mhlanga, S. D.; Mondal, K. C.; Carter, R.; Witcomb, M. J.; Coville, N. J., The effect of synthesis parameters on the catalytic synthesis of multiwalled carbon nanotubes using Fe-Co/CaCO<sub>3</sub> catalysts. *South African Journal of Chemistry* **2009**, 62, 67-76.

21. Li, Q.; Yan, H.; Zhang, J.; Liu, Z., Effect of hydrocarbons precursors on the formation of carbon nanotubes in chemical vapor deposition. *Carbon* **2004**, 42, (4),

829-835.

22. Shah, K. A.; Tali, B. A., Synthesis of carbon nanotubes by catalytic chemical vapour deposition: A review on carbon sources, catalysts and substrates. *Materials Science in Semiconductor Processing* **2016**, 41, 67-82.
23. Stobinski, L.; Lesiak, B.; Kövér, L.; Tóth, J.; Biniak, S.; Trykowski, G.; Judek, J., Multiwall carbon nanotubes purification and oxidation by nitric acid studied by the FTIR and electron spectroscopy methods. *Journal of Alloys and Compounds* **2010**, 501, (1), 77-84.
24. Ren, Z. F.; Huang, Z. P.; Xu, J. W.; Wang, J. H.; Bush, P.; Siegal, M. P.; Provencio, P. N., Synthesis of large arrays of well-aligned carbon nanotubes on glass. *Science* **1998**, 282, (5391), 1105-7.
25. Che, G.; Lakshmi, B. B.; Martin, C. R.; Fisher, E. R.; Ruoff, R. S., Chemical Vapor Deposition Based Synthesis of Carbon Nanotubes and Nanofibers Using a Template Method. *Chemistry of Materials* **1998**, 10, (1), 260-267.
26. Hou, P.; Liu, C.; Shi, C.; Cheng, H., Carbon nanotubes prepared by anodic aluminum oxide template method. *Chinese Science Bulletin* **2012**, 57, (2), 187-204.
27. Jeong, S.-H.; Hwang, H.-Y.; Hwang, S.-K.; Lee, K.-H., Carbon nanotubes based on anodic aluminum oxide nano-template. *Carbon* **2004**, 42, (10), 2073-2080.
28. Mijangos, C.; Hernández, R.; Martín, J., A review on the progress of polymer nanostructures with modulated morphologies and properties, using nanoporous AAO templates. *Progress in Polymer Science* **2016**, 54–55, 148-182.
29. Kyotani, T.; Tsai, L.-f.; Tomita, A., Preparation of Ultrafine Carbon Tubes in

Nanochannels of an Anodic Aluminum Oxide Film. *Chemistry of Materials* **1996**, 8, (8), 2109-2113.

30. Chen, J. T.; Shin, K.; Leiston-Belanger, J. M.; Zhang, M.; Russell, T. P., Amorphous Carbon Nanotubes with Tunable Properties via Template Wetting. *Advanced Functional Materials* **2006**, 16, (11), 1476-1480.

31. Golshadi, M.; Maita, J.; Lanza, D.; Zeiger, M.; Presser, V.; Schrlau, M. G., Effects of synthesis parameters on carbon nanotubes manufactured by template-based chemical vapor deposition. *Carbon* **2014**, 80, 28-39.

32. Mehrnia, M. R.; Mojtahedi, Y. M.; Homayoonfal, M., What is the concentration threshold of nanoparticles within the membrane structure? A case study of Al<sub>2</sub>O<sub>3</sub>/PSf nanocomposite membrane. *Desalination* **2015**, 372, (Supplement C), 75-88.

33. Tapsuan, K.; Niyomwas, S., Effect of Preform Conditions on Synthesis of Fe<sub>3</sub>Al-TiB<sub>2</sub>- Al<sub>2</sub>O<sub>3</sub> Composite by Self-Propagating High-Temperature Synthesis. *Procedia Engineering* **2012**, 32, (Supplement C), 635-641.

34. Sui, Y. C.; Cui, B. Z.; Guardián, R.; Acosta, D. R.; Martínez, L.; Perez, R., Growth of carbon nanotubes and nanofibres in porous anodic alumina film. *Carbon* **2002**, 40, (7), 1011-1016.

35. Wu, C.; Wang, L.; Williams, P. T.; Shi, J.; Huang, J., Hydrogen production from biomass gasification with Ni/MCM-41 catalysts: Influence of Ni content. *Applied Catalysis B: Environmental* **2011**, 108–109, 6-13.

36. Liu, X.; Zhang, Y.; Nahil, M. A.; Williams, P. T.; Wu, C., Development of Ni- and Fe- based catalysts with different metal particle sizes for the production of carbon

nanotubes and hydrogen from thermo-chemical conversion of waste plastics. *Journal of Analytical and Applied Pyrolysis*.

37. Wu, C.; Nahil, M. A.; Norbert, M.; Huang, J.; Williams, P. T., Production and application of carbon nanotubes, as a co-product of hydrogen from the pyrolysis-catalytic reforming of waste plastic. *Process Safety and Environmental Protection*.

38. Jiang, B.; Zhang, C.; Wang, K.; Dou, B.; Song, Y.; Chen, H.; Xu, Y., Highly dispersed Ni/montmorillonite catalyst for glycerol steam reforming: Effect of Ni loading and calcination temperature. *Applied Thermal Engineering* **2016**, 109, Part A, 99-108.

39. Richardson, J. T.; Crump, J. G., Crystallite size distributions of sintered nickel catalysts. *Journal of Catalysis* **1979**, 57, (3), 417-425.

40. Wu, C.; Williams, P. T., Investigation of Ni-Al, Ni-Mg-Al and Ni-Cu-Al catalyst for hydrogen production from pyrolysis-gasification of polypropylene. *Applied Catalysis B: Environmental* **2009**, 90, (1-2), 147-156.

41. Gorbunov, A.; Jost, O.; Pompe, W.; Graff, A., Role of the catalyst particle size in the synthesis of single-wall carbon nanotubes. *Applied Surface Science* **2002**, 197-198, 563-567.

42. Cheung, C. L.; Kurtz, A.; Park, H.; Lieber, C. M., Diameter-Controlled Synthesis of Carbon Nanotubes. *The Journal of Physical Chemistry B* **2002**, 106, (10), 2429-2433.

43. Chen, D.; Christensen, K. O.; Ochoa-Fernández, E.; Yu, Z.; Tøtdal, B.; Latorre, N.; Monzón, A.; Holmen, A., Synthesis of carbon nanofibers: effects of Ni crystal size during methane decomposition. *Journal of Catalysis* **2005**, 229, (1), 82-96.

44. Sinnott, S. B.; Andrews, R.; Qian, D.; Rao, A. M.; Mao, Z.; Dickey, E. C.; Derbyshire, F., Model of carbon nanotube growth through chemical vapor deposition. *Chemical Physics Letters* **1999**, 315, (1–2), 25-30.
45. Takenaka, S.; Serizawa, M.; Otsuka, K., Formation of filamentous carbons over supported Fe catalysts through methane decomposition. *Journal of Catalysis* **2004**, 222, (2), 520-531.
46. Lee, C. J.; Park, J.; Yu, J. A., Catalyst effect on carbon nanotubes synthesized by thermal chemical vapor deposition. *Chemical Physics Letters* **2002**, 360, (3–4), 250-255.
47. Liu, J.; Jiang, Z. W.; Yu, H. O.; Tang, T., Catalytic pyrolysis of polypropylene to synthesize carbon nanotubes and hydrogen through a two-stage process. *Polymer Degradation and Stability* **2011**, 96, (10), 1711-1719.
48. Nahil, M. A.; Wu, C.; Williams, P. T., Influence of metal addition to Ni-based catalysts for the co-production of carbon nanotubes and hydrogen from the thermal processing of waste polypropylene. *Fuel Processing Technology* **2015**, 130, 46-53.
49. Namioka, T.; Saito, A.; Inoue, Y.; Park, Y.; Min, T. J.; Roh, S. A.; Yoshikawa, K., Hydrogen-rich gas production from waste plastics by pyrolysis and low-temperature steam reforming over a ruthenium catalyst. *Applied Energy* **2011**, 88, (6), 2019-2026.
50. Kumar, M.; Ando, Y., Controlling the diameter distribution of carbon nanotubes grown from camphor on a zeolite support. *Carbon* **2005**, 43, (3), 533-540.
51. Aqel, A.; El-Nour, K. M. M. A.; Ammar, R. A. A.; Al-Warthan, A., Carbon nanotubes, science and technology part (I) structure, synthesis and characterisation.

*Arabian Journal of Chemistry* **2012**, 5, (1), 1-23.

52. Danafar, F.; Fakhru'l-Razi, A.; Salleh, M. A. M.; Biak, D. R. A., Fluidized bed catalytic chemical vapor deposition synthesis of carbon nanotubes—A review.

*Chemical Engineering Journal* **2009**, 155, (1–2), 37-48.

53. Stoner, B. R.; Brown, B.; Glass, J. T., Selected Topics on the Synthesis, Properties and Applications of Multiwalled Carbon Nanotubes. *Diam Relat Mater* **2014**, 42, 49-57.

54. Niu, J. J.; Wang, J. N.; Jiang, Y.; Su, L. F.; Ma, J., An approach to carbon nanotubes with high surface area and large pore volume. *Microporous and Mesoporous Materials* **2007**, 100, (1–3), 1-5.

55. Kukovecz, A.; Konya, Z.; Nagaraju, N.; Willems, I.; Tamasi, A.; Fonseca, A.; Nagy, J. B.; Kiricsi, I., Catalytic synthesis of carbon nanotubes over Co, Fe and Ni containing conventional and sol-gel silica-aluminas. *Physical Chemistry Chemical Physics* **2000**, 2, (13), 3071-3076.

56. Kathyayini, H.; Willems, I.; Fonseca, A.; Nagy, J. B.; Nagaraju, N., Catalytic materials based on aluminium hydroxide, for the large scale production of bundles of multi-walled (MWNT) carbon nanotubes. *Catalysis Communications* **2006**, 7, (3), 140-147.

57. Smajda, R.; Kukovecz, Á.; Kónya, Z.; Kiricsi, I., Structure and gas permeability of multi-wall carbon nanotube buckypapers. *Carbon* **2007**, 45, (6), 1176-1184.

58. Li, W. Z.; Wen, J. G.; Ren, Z. F., Effect of temperature on growth and structure of carbon nanotubes by chemical vapor deposition. *Applied Physics A* **2002**, 74, (3), 397-

402.

59. Futaba, D. N.; Hata, K.; Yamada, T.; Mizuno, K.; Yumura, M.; Iijima, S., Kinetics of Water-Assisted Single-Walled Carbon Nanotube Synthesis Revealed by a Time-Evolution Analysis. *Physical Review Letters* **2005**, 95, (5), 056104.

60. Acomb, J. C.; Wu, C.; Williams, P. T., The use of different metal catalysts for the simultaneous production of carbon nanotubes and hydrogen from pyrolysis of plastic feedstocks. *Applied Catalysis B: Environmental* **2016**, 180, 497-510.

61. Barbarias, I.; Lopez, G.; Amutio, M.; Artetxe, M.; Alvarez, J.; Arregi, A.; Bilbao, J.; Olazar, M., Steam reforming of plastic pyrolysis model hydrocarbons and catalyst deactivation. *Applied Catalysis A: General* **2016**, 527, 152-160.

62. Hata, K.; Futaba, D. N.; Mizuno, K.; Namai, T.; Yumura, M.; Iijima, S., Water-assisted highly efficient synthesis of impurity-free single-walled carbon nanotubes. *Science* **2004**, 306, (5700), 1362-4.

63. Ago, H.; Uehara, N.; Yoshihara, N.; Tsuji, M.; Yumura, M.; Tomonaga, N.; Setoguchi, T., Gas analysis of the CVD process for high yield growth of carbon nanotubes over metal-supported catalysts. *Carbon* **2006**, 44, (14), 2912-2918.

64. Donatelli, A.; Iovane, P.; Molino, A., High energy syngas production by waste tyres steam gasification in a rotary kiln pilot plant. Experimental and numerical investigations. *Fuel* **2010**, 89, (10), 2721-2728.

65. Lee, K.-Y.; Yeoh, W.-M.; Chai, S.-P.; Ichikawa, S.; Mohamed, A. R., The role of water vapor in carbon nanotube formation via water-assisted chemical vapor deposition of methane. *Journal of Industrial and Engineering Chemistry* **2012**, 18, (4), 1504-1511.

66. Liu, H.; Zhang, Y.; Li, R.; Sun, X.; Wang, F.; Ding, Z.; Mérel, P.; Desilets, S., Aligned synthesis of multi-walled carbon nanotubes with high purity by aerosol assisted chemical vapor deposition: Effect of water vapor. *Applied Surface Science* **2010**, 256, (14), 4692-4696.
67. Hu, J. L.; Yang, C. C.; Huang, J. H., Vertically-aligned carbon nanotubes prepared by water-assisted chemical vapor deposition. *Diamond and Related Materials* **2008**, 17, (12), 2084-2088.
68. Yamada, T.; Maigne, A.; Yudasaka, M.; Mizuno, K.; Futaba, D. N.; Yumura, M.; Iijima, S.; Hata, K., Revealing the Secret of Water-Assisted Carbon Nanotube Synthesis by Microscopic Observation of the Interaction of Water on the Catalysts. *Nano Letters* **2008**, 8, (12), 4288-4292.

**Table 1 X-ray diffraction crystallite size measurements of NiO**

|                              | <i>0.1 / AAO</i> | <i>0.5 / AAO</i> | <i>1.0 / AAO</i> | <i>2.0 / AAO</i> |
|------------------------------|------------------|------------------|------------------|------------------|
| <i>Crystallite size / nm</i> | ----             | 32.6             | 36.9             | 47.7             |

**Table 2 – Overall view of experiments parameters and carbon depositions**

|                                     | Ni Content<br>( $\text{molL}^{-1}$ ) | Temperature<br>( $^{\circ}\text{C}$ ) | Steam<br>addition<br>(mL) | Amorphous<br>Carbon<br>(%) | Filamentous<br>Carbon<br>(%) | CNTs Average<br>Diameter<br>(nm) |
|-------------------------------------|--------------------------------------|---------------------------------------|---------------------------|----------------------------|------------------------------|----------------------------------|
| <i>Effect of the<br/>Ni content</i> | 0.1                                  | 700                                   |                           | 2.5                        | 7.5                          | 26.7 ± 4.0                       |
|                                     | 0.5                                  | 700                                   |                           | 1.2                        | 5.3                          | 38.3 ± 14.2                      |
|                                     | 1.0                                  | 700                                   |                           | 3.0                        | 22.0                         | 40.1 ± 11.5                      |
|                                     | 2.0                                  | 700                                   |                           | 3.0                        | 20.5                         | 54.1 ± 7.5                       |
| <i>Effect of<br/>temperature</i>    | 0.1                                  | 600                                   |                           | 1.2                        | 1.8                          | 26.2 ± 6.6                       |
|                                     | 0.1                                  | 700                                   |                           | 1.1                        | 4.7                          | 33.5 ± 5.6                       |
|                                     | 0.1                                  | 800                                   |                           | -                          | -                            | 27.2 ± 7.2                       |
| <i>Effect of steam<br/>addition</i> | 0.1                                  | 700                                   | 0                         | 1.7                        | 3.3                          | 33.5 ± 5.6                       |
|                                     | 0.1                                  | 700                                   | 2                         | 1.7                        | 1.1                          | 29.2 ± 5.7                       |
|                                     | 0.1                                  | 700                                   | 5                         | 2.2                        | 7.5                          | 21.9 ± 3.9                       |

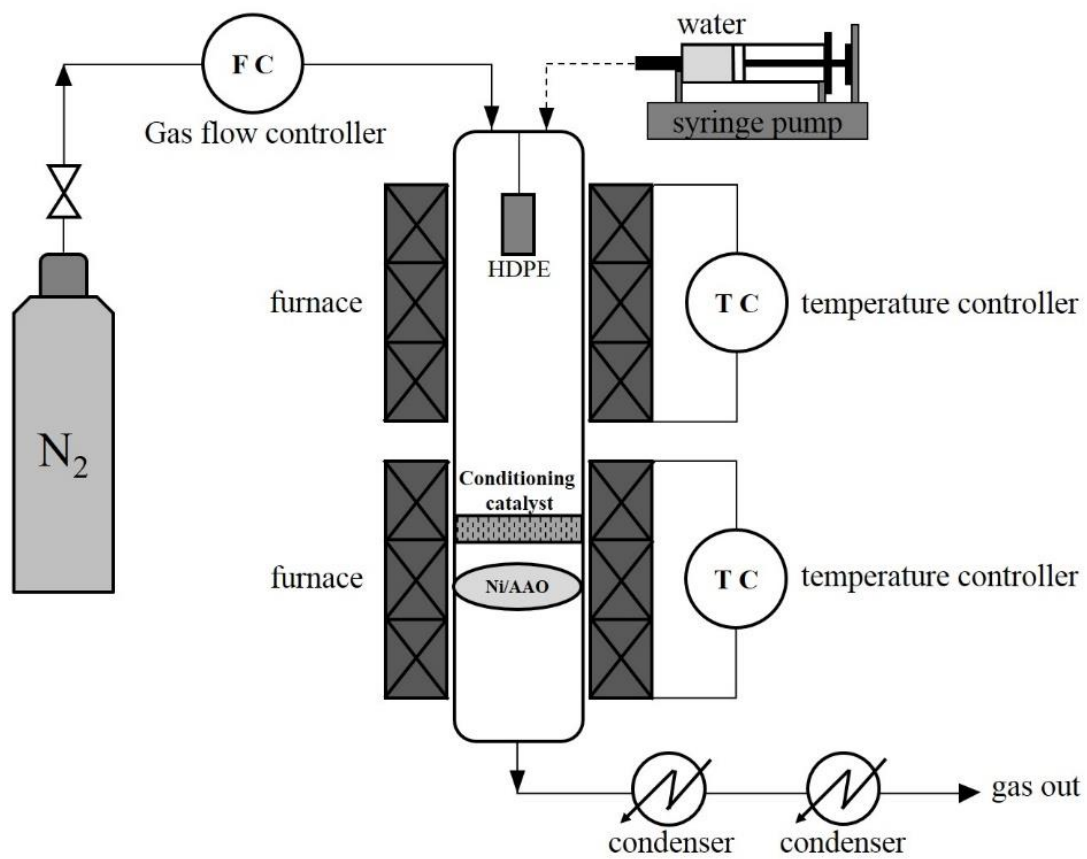


Fig. 1 Schematic diagram of the two-stage fixed bed reactor for the synthesis of CNTs from waste plastics

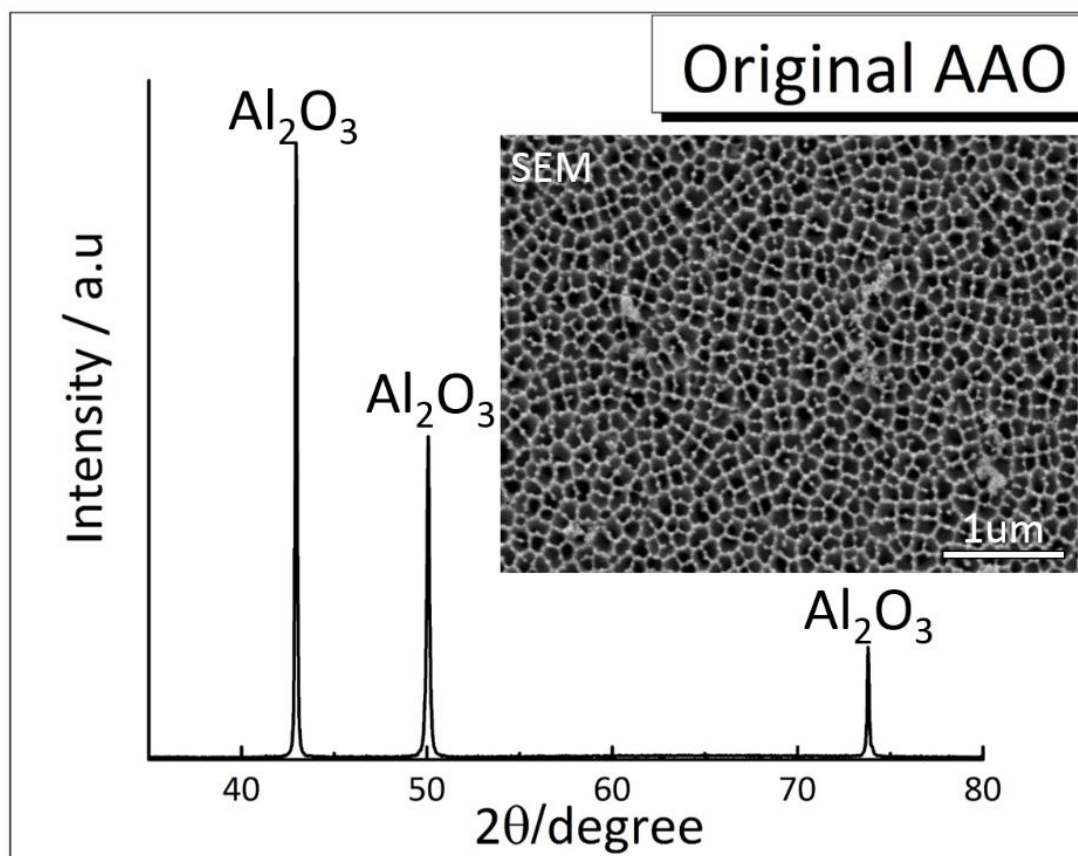


Fig. 2 XRD results for original AAO membrane without Ni loading, and surface SEM image

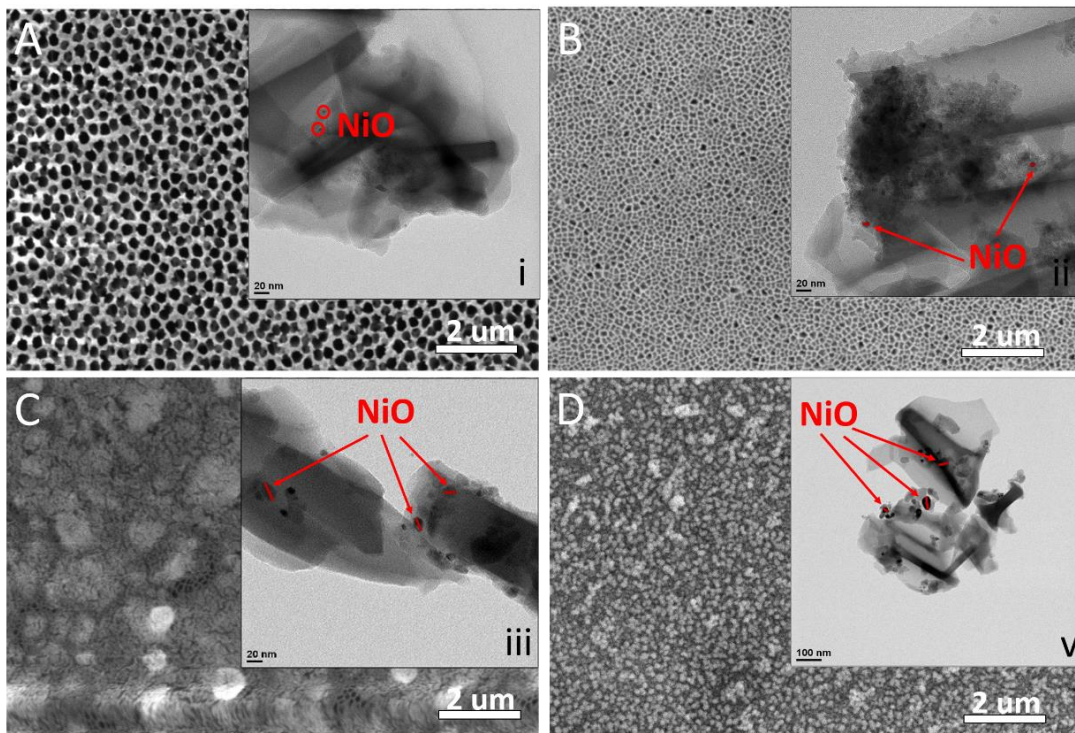


Fig. 3 SEM (A-D) and TEM (i-v) results for fresh 0.1/AAO, 0.5/AAO, 1.0/AAO, and 2.0/AAO catalysts

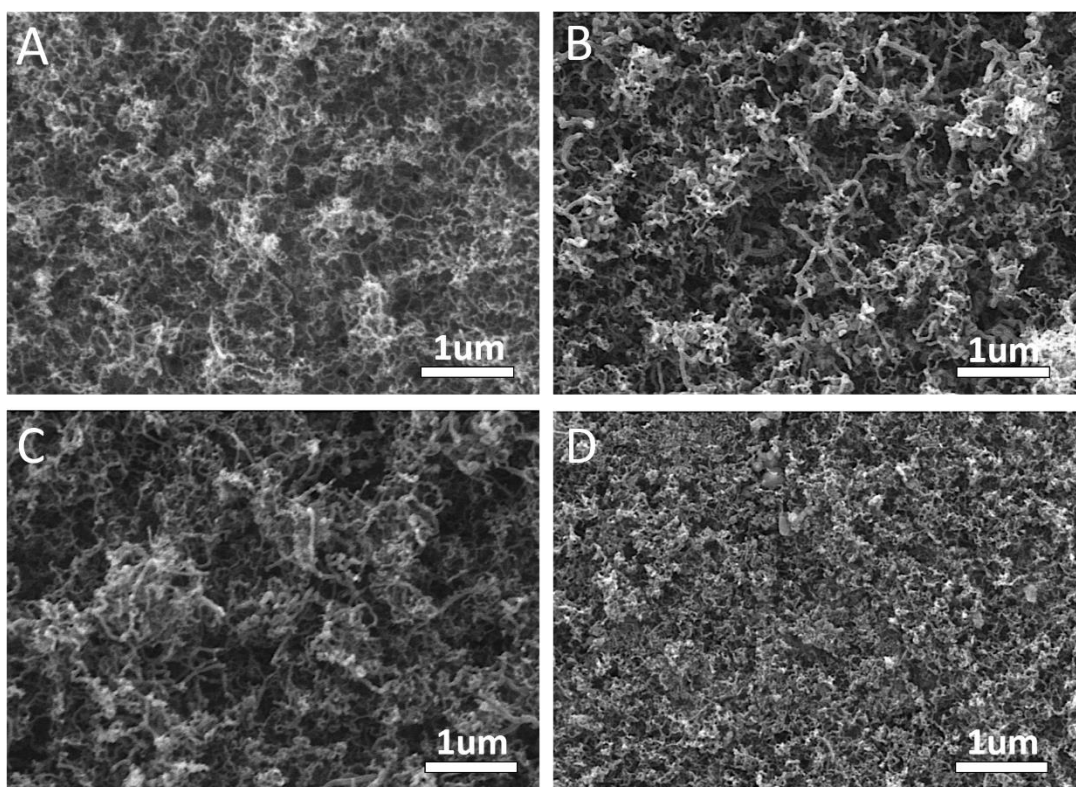


Fig. 4 SEM results of the reacted Ni/AAO catalyst (A) 0.1/AAO; (B) 0.5/AAO; (C) 1.0/AAO and (D) 2.0/AAO

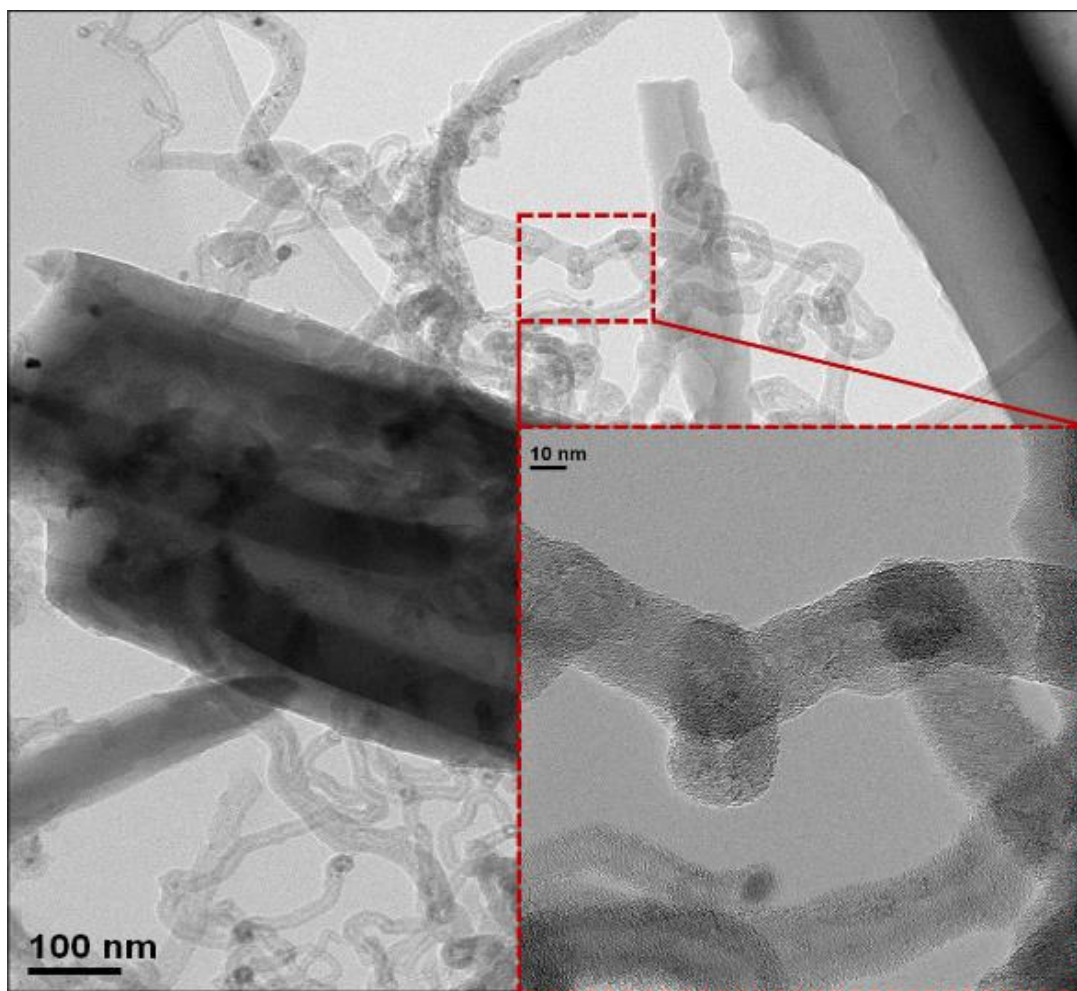


Fig. 5 TEM results of CNTs for the reacted 0.1/AAO catalyst at different magnification

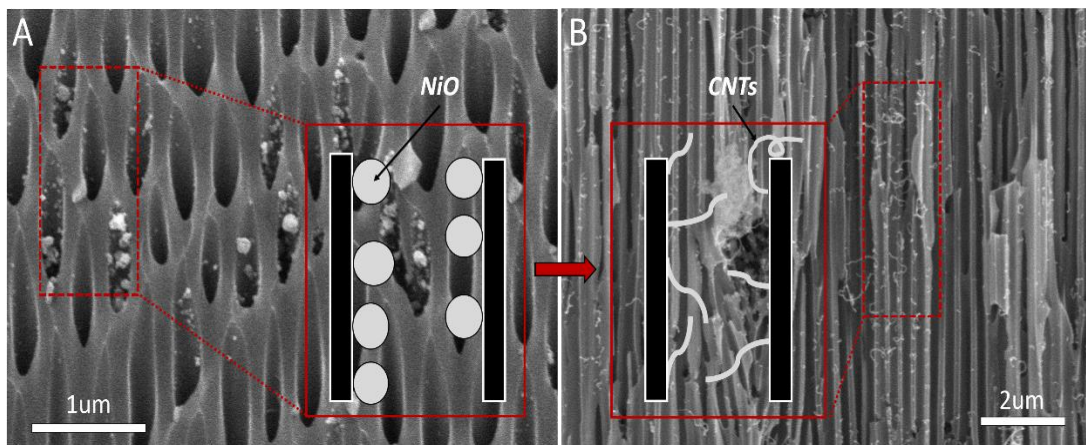


Fig. 6 Mechanisms of CNTs growth using Ni/AAO membrane catalyst

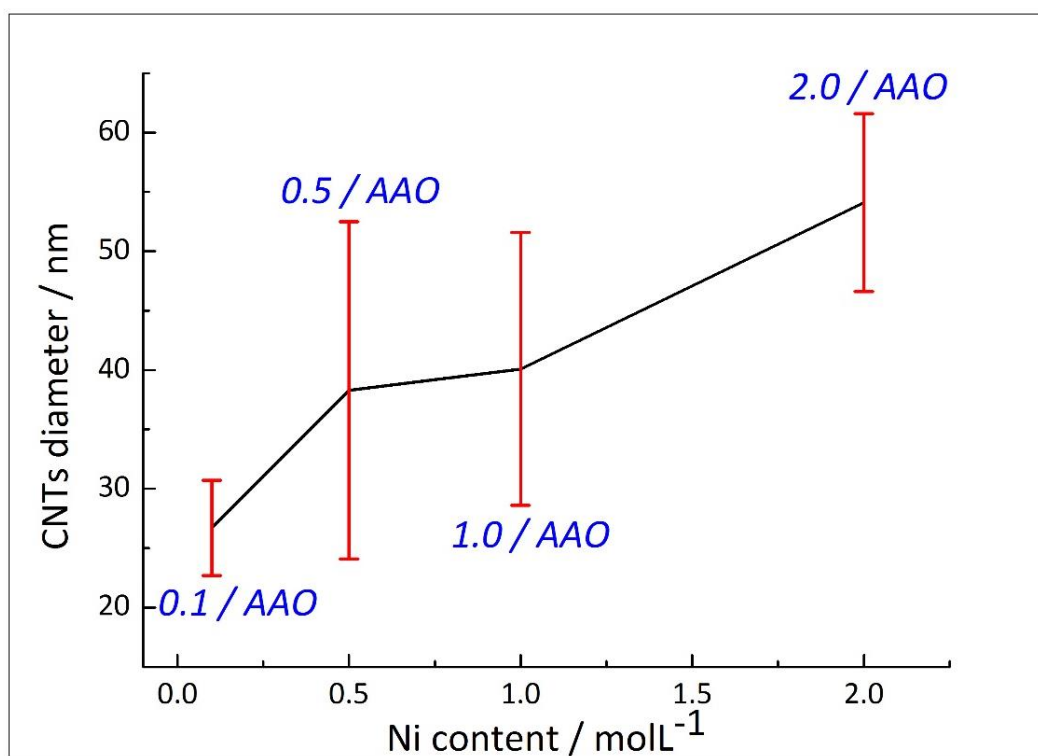


Fig. 7 CNTs diameter distribution for different contents of AAO membrane catalysts

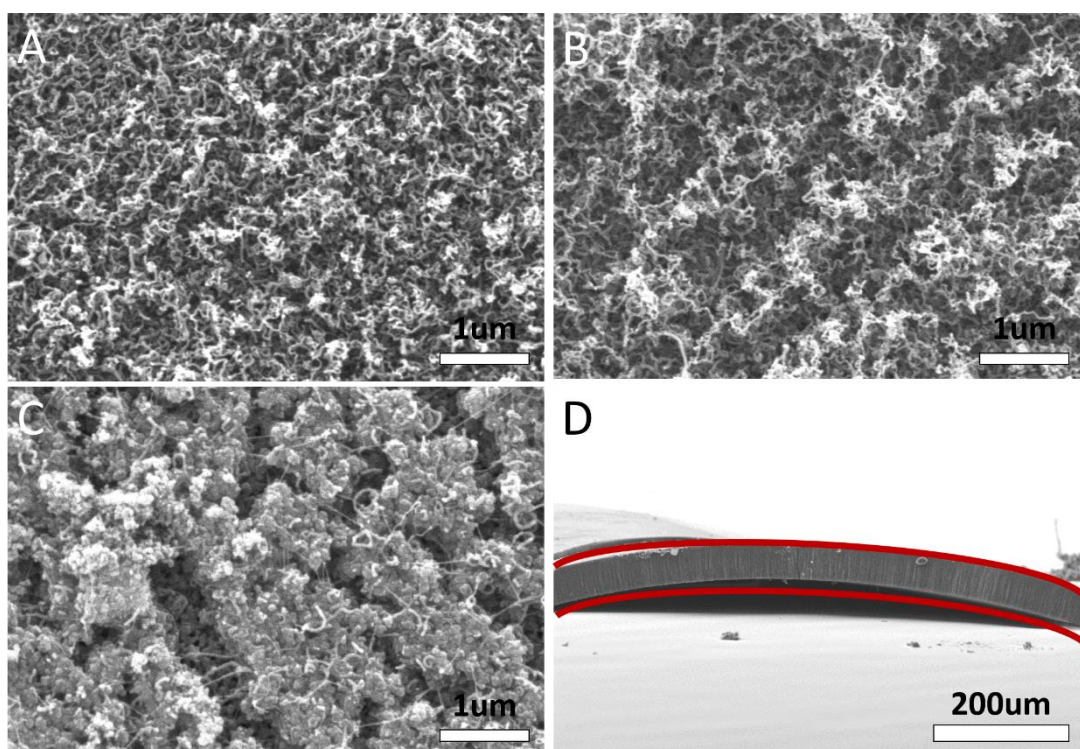


Fig. 8 SEM results of 0.1/AAO catalyst for CNTs growth at different temperatures. (A) 600 °C; (B) 700 °C; (C) 800 °C; and (D) cross-section for cracking boundary at 800 °C

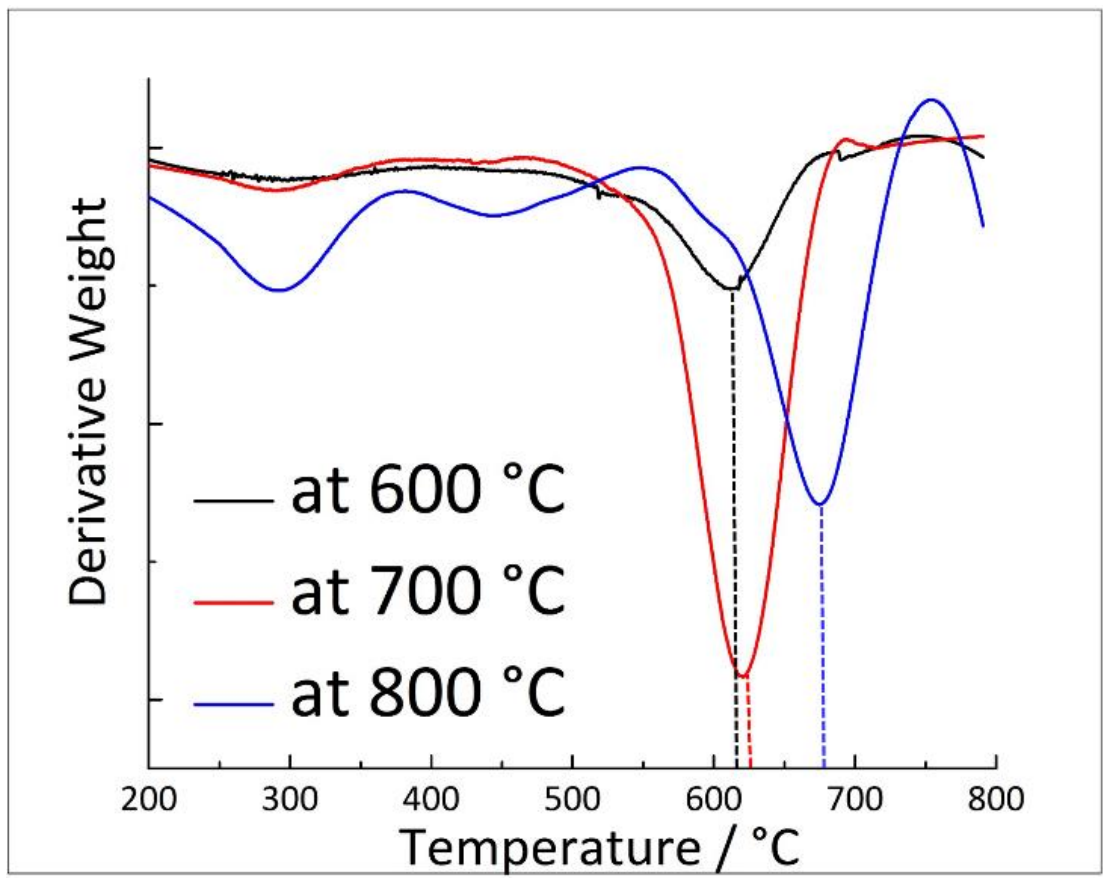


Fig. 9 DTG-TPO results of the reacted 0.1/AAO catalyst tested at 600 °C, 700 °C and 800 °C

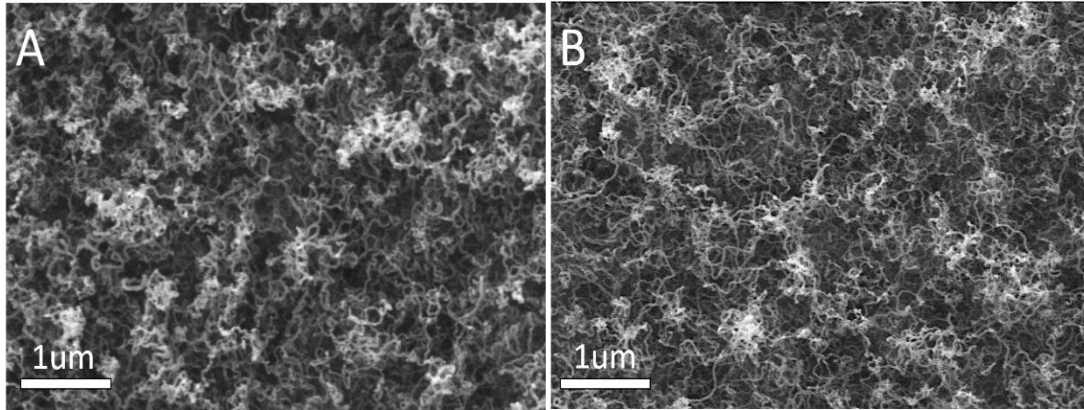


Fig. 10 SEM results of the reacted 0.1/AAO catalyst at 700 °C with different rate of steam injected. (A) 2 mL h<sup>-1</sup> and (B) 5 mL h<sup>-1</sup>

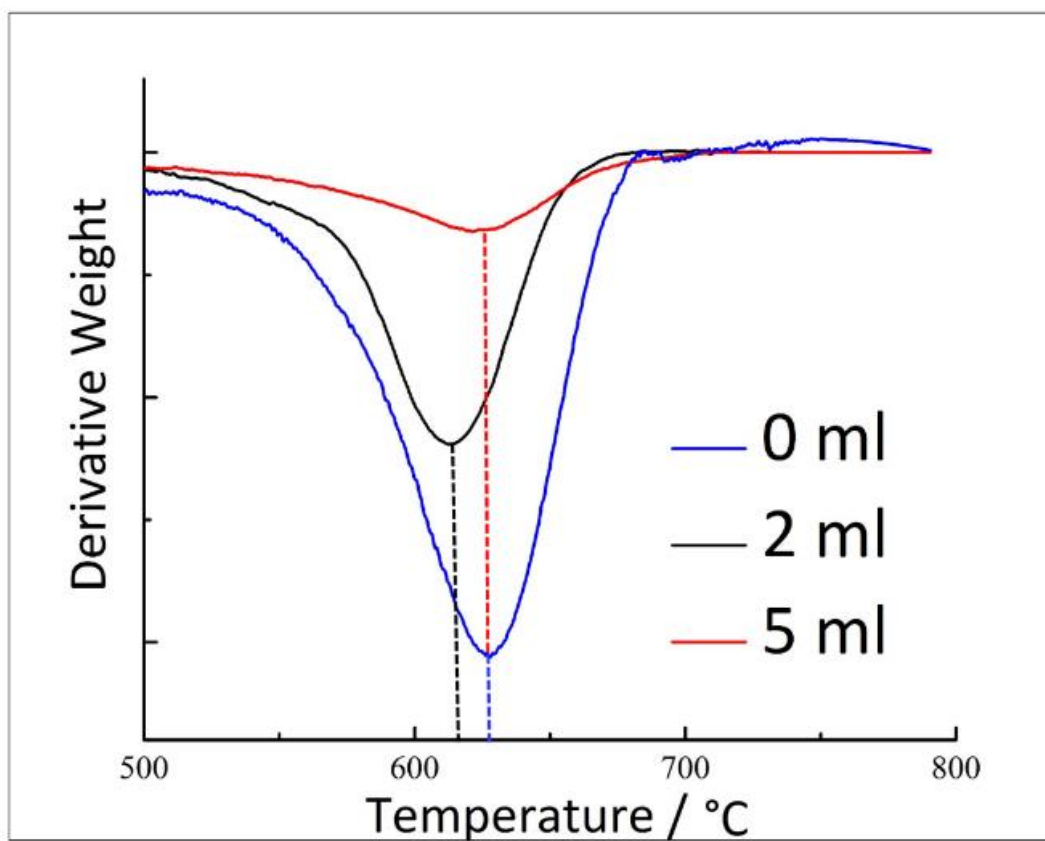


Fig. 11 DTG-TPO results of the reacted 0.1/AAO catalyst tested with 0, 2 and 5 mL h<sup>-1</sup> steam injection